



Photocatalytic oxidation of NO_x over TiO₂/HZSM-5 catalysts in the presence of water vapor: Effect of hydrophobicity of zeolites

Gaofei Guo, Yun Hu*, Shumei Jiang, Chaohai Wei

The Key Lab of Pollution Control and Ecosystem Restoration in Industry Clusters, Ministry of Education, College of Environmental Science and Engineering, South China University of Technology, Guangzhou 510006, PR China

ARTICLE INFO

Article history:

Received 8 November 2011
Received in revised form 13 April 2012
Accepted 17 April 2012
Available online 24 April 2012

Keywords:

Photocatalysis
NO_x oxidation
TiO₂
HZSM-5 zeolites
Water vapor

ABSTRACT

TiO₂ hybridized with HZSM-5 zeolites photocatalysts were prepared by a simple solid state dispersion method. The physicochemical properties of the catalysts were characterized by X-ray diffraction, UV–vis diffuse reflectance and FT-IR spectroscopy. The photocatalytic oxidation of NO_x over TiO₂/HZSM-5 having different Si/Al ratios was carried out under various levels of humidity and different pre-adsorption times in dark. The TiO₂/HZSM-5 composite catalysts exhibited higher NO conversion and lower NO₂ formation than pure TiO₂. Pre-adsorption with water vapor and the high humidity during the photoreaction were harmful to the reactivity of TiO₂ hybridized with hydrophilic HZSM-5 zeolite. However, the photocatalytic reactivity of TiO₂ hybridized with hydrophobic zeolite varied little with increase in humidity. The results indicated that the high photocatalytic reactivity of TiO₂/HZSM-5 catalysts is largely depended on the hydrophobicity of the zeolites.

© 2012 Elsevier B.V. All rights reserved.

1. Introduction

Nitrogen oxides (NO_x), which emitted largely from automobiles and electric utilities, are major contributors to air pollution such as acid rain and photochemical smog. Photocatalysis is an attractive approach for environmental remediation [1–5]. The photocatalytic oxidation of NO involves a series of steps by HO• radicals: NO → HNO₂ → NO₂ → HNO₃ [6,7]. As one of the most popular photocatalysts, titanium dioxide has attracted extensive interests due to its distinct properties like chemical stability, high reactivity and non-toxicity. However, the removal efficiency of air pollutants in TiO₂-based systems is generally low, because conventional TiO₂ photocatalysts have small surface area that cannot efficiently adsorb pollutants diffused in wide spaces [8]. It is known that Degussa P25 has a high photocatalytic activity under UV light irradiation, but it has a small Brunauer–Emmett–Teller (BET) surface area (around 55 m²/g) [9]. Therefore, there is a necessity to improve the surface area of TiO₂ so that the photocatalytic activity can be considerably enhanced. For this purpose, many researchers focus on improving surface area by loading TiO₂ onto porous adsorbents such as molecular sieves [10–13] and active carbon [14], or by preparing mesoporous TiO₂ [15,16]. However, the porous materials, especially microporous zeolites, can not only adsorb target pollutants, but also show strong affinity for water vapor, even at

low partial pressure of water [17]. In many cases, water vapor plays a dual role in the photocatalytic reaction. On one hand, it serves as HO• radical supplier by photo-induced holes which are responsible for oxidative attacks [18,19]. On the other hand, as an adsorption inhibitor it competes with target pollutants [20–22] which can decrease the contact efficiency between target pollutants and active sites, followed by a negative effect on photoefficiency. Anyhow, the photocatalytic oxidation of atmosphere pollutants at high humidity levels is a challenge for practical application due to the negative effects of water vapor on photocatalytic activity.

The photocatalytic oxidation activity of NO_x over titania–zeolite composites outperform pure TiO₂ in the absence of water vapor [11,23]. It has been reported that highly siliceous ZSM-5 zeolites with high Si/Al ratios have highly hydrophobic surfaces [17]. To improve the photocatalytic oxidation efficiency of NO_x in the presence of water vapor, we hybridized the ZSM-5 having different Si/Al ratios with TiO₂ by a simple solid state dispersion (SSD) method in this work. A crucial question concerning ZSM-5 hybridized with TiO₂ photocatalysts is how the water vapor influences the photocatalytic oxidation of NO_x under alternative hydrophobic or hydrophilic zeolite. From this standpoint, the effects of water vapor related to adsorption time in dark and different levels of humidity on zeolites for photocatalytic oxidation of NO_x over ZSM-5 hybridized with TiO₂ composites were investigated in detail by transient behavior. Various spectroscopic techniques such as UV–vis, XRD and FT-IR spectroscopy were applied to characterize the photocatalysts. To our best knowledge, the effects of different humidity and adsorption time in dark on photocatalytic oxidation

* Corresponding author. Tel.: +86 20 39380573; fax: +86 20 39380588.
E-mail address: huyun@scut.edu.cn (Y. Hu).

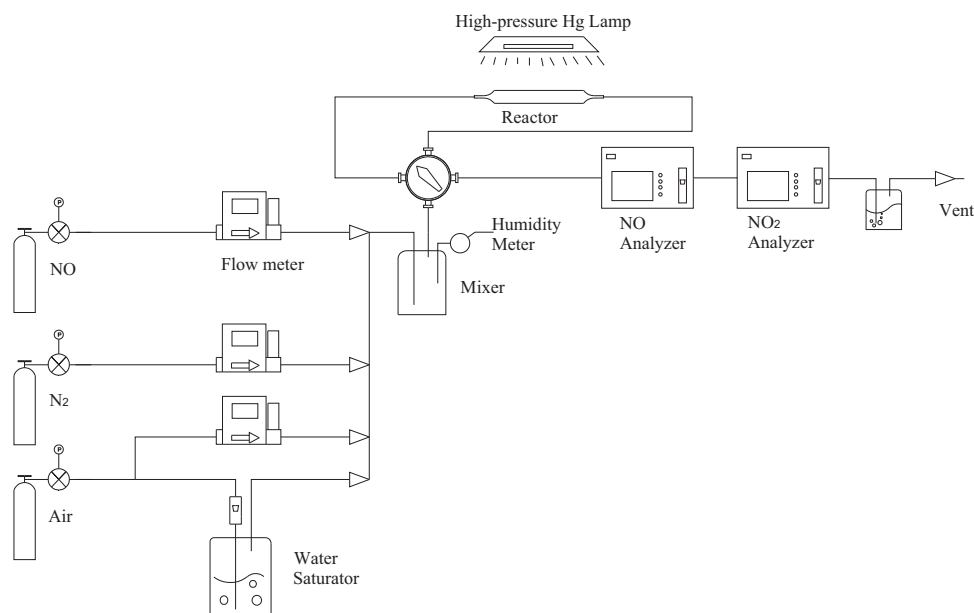


Fig. 1. Schematic diagram of the photocatalytic oxidation equipment.

of NO_x over TiO_2 hybridized with ZSM-5 zeolites have not been reported yet.

2. Experimental

2.1. Catalysts preparation

Various ZSM-5 zeolite samples were obtained from The Catalyst Plant of Naikai University. The ZSM-5 zeolites with Si/Al ratios of 500, 200 and 25 were supplied as the H^+ -type zeolite, namely HZSM-5. Before the experiments, the HZSM-5 zeolites were calcined in air at 723 K for 4 h. HZSM-5 hybridized with TiO_2 complex having different TiO_2 contents were prepared by a SSD method [24]. Initially, TiO_2 (P25, crystal size: 30–50 nm, Degussa Co., Ltd.) was mixed thoroughly with HZSM-5 (with Si/Al ratios of 500, 200 and 25) using ethanol as a dispersing agent in an agate mortar, and then the mixture was blended for 45 min. After that, the mixed solids were calcined in air at 723 K for 3 h to obtain $\text{TiO}_2/\text{HZSM-5}$ with Si/Al ratios of 500, 200 and 25, respectively. The corresponding zeolite content was adjusted to 80, 60 and 40 wt%, respectively.

2.2. Catalysts characterizations

The X-ray diffraction (XRD) patterns of the powder samples were recorded with a D8 Advance (Bruker AXS, Germany) diffractometer using $\text{Cu K}\alpha$ radiation ($\lambda = 1.5406 \text{ \AA}$). Diffuse reflectance UV–vis spectroscopic measurements were performed on a Shimadzu UV–vis spectrophotometer UV-2550, and BaSO_4 was used as a reference sample. Specific surface area was obtained from N_2 adsorption–desorption isotherms at 77 K (Micromeritics ASAP 2020M Analysis). Surface area was calculated by the BET method. The FT-IR spectra were obtained with a resolution of 4 cm^{-1} at 298 K on a Nicolet 6700 spectrometer using KBr-pellet technique (0.67 wt% zeolite in a KBr matrix), and the spectra were recorded in the region of $4000\text{--}400 \text{ cm}^{-1}$. SEM images were taken with a scanning electron microscope (SEM, ZEISS EVO LS10).

2.3. Photocatalytic activity measurement

The photocatalytic oxidation of NO_x was performed at an ambient temperature under a continuous flow reactor. The

experimental setup is shown in Fig. 1. By mixing NO, N_2 and wet air streams to obtain the desired concentration (40–45 ppm) and humidity, the flow rate was controlled at 200 mL min^{-1} . The inner volume of the rectangular reactor made of quartz was 4.5 mL ($5 \text{ mm} \times 60 \text{ mm} \times 15 \text{ mm}$ ($H \times L \times W$)). The space velocity of gas in the continuous flow reactor was 0.68 s^{-1} . The powders of samples were dispersed onto the bottom of the reactor and the amount of TiO_2 was constant at 20 mg for each experiment. A 125 W high pressure mercury lamp (Philips) was used for UV light source. Two fans were used to prevent the rise of temperature in the flow system. The UV light intensity of 365 nm was 1.6 mW cm^{-2} and measured with a UVA radiometer (Photoelectric Instrument Factory of Beijing Normal University). The concentration of NO and NO_2 was continuously measured by an infrared spectrum analyzer (GXH-1050E, Beijing Junfang Co., Ltd.) and an electrochemical analyzer (GXH-1050E, Beijing Junfang Co., Ltd.), respectively. Adsorption time in dark was defined as the time of the gas stream contact with photocatalysts before irradiation.

Blank tests were carried out using a mixed reactants flow involving 40 ppm inlet NO under UV light irradiation without the $\text{TiO}_2/\text{HZSM-5}$ photocatalysts and with HZSM-5 only at room temperature, respectively. The variation of the NO and NO_2 concentration could not be observed. Moreover, there was no change of the NO and NO_2 concentration when the lamp was turned off and the catalysts were present in the reactor.

3. Results and discussion

3.1. Characterization of catalysts

As far as the microporous support is concerned, Table 1 shows the surface area of HZSM-5 with different Si/Al ratios, suggesting that Si/Al ratio has no significant harmful effect on architecture of

Table 1
BET surface area of HZSM-5 with different Si/Al ratios.

Si/Al	BET SA ($\text{m}^2 \text{ g}^{-1}$)
25	344.6
200	335.8
500	352.8

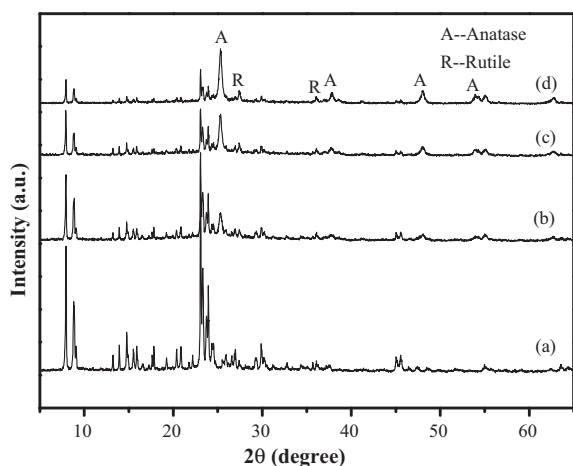


Fig. 2. XRD patterns of the samples with different zeolite contents. (a) HZSM-5; (b) TiO₂/HZSM-5(500) 80 wt%; (c) TiO₂/HZSM-5(500) 60 wt%; (d) TiO₂/HZSM-5(500) 40 wt%.

HZSM-5. The mean pore size of HZSM-5 is 0.55 nm (obtained from The Catalyst Plant of Naikai University). Fig. 2 shows the XRD patterns of the samples prepared by the SSD method with different zeolite contents. All the samples showed diffraction patterns (typically at low-angle ($2\theta < 10^\circ$)) for the HZSM-5 zeolite which could be assigned to a MFI structure, suggesting that the preparation method has little effect on the architecture of the zeolite. With the increase in the TiO₂ content, the intensity of diffraction patterns for the zeolite decreased, while the intensity of the diffraction peak at around 25.4° (2θ) attributed to the anatase (1 0 1) phase increased, suggesting that TiO₂ homogeneously dispersed on the surface of the HZSM-5 zeolite [25]. The effects of different Si/Al ratios of HZSM-5 on the XRD patterns of samples are shown in Fig. 3. It was found that the crystallinity of the zeolites was enhanced at lower aluminum contents, which was consistent with the result reported by M.A. Ali et al. [26], suggesting that excess amount of Al is unfavorable to crystallinity.

Fig. 4 shows SEM images of the TiO₂ hybridized with HZSM-5 zeolite (TiO₂/HZSM-5(500) 60 wt%). As shown in Fig. 4, TiO₂ particles were dispersed on the surfaces of zeolite, supporting the truth that TiO₂ well dispersed onto zeolite suggested by X-ray diffraction. Fig. 5 depicts the UV–vis diffuse reflectance spectra of the samples with different zeolite contents. With the content of zeolite in TiO₂/HZSM-5 increased, the absorption band of TiO₂ decreased

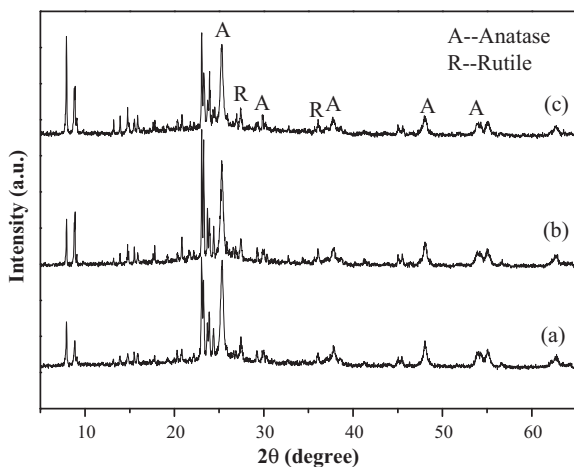


Fig. 3. XRD patterns of the samples with different Si/Al ratios. (a) TiO₂/HZSM-5(25) 60 wt%; (b) TiO₂/HZSM-5(200) 60 wt%; (c) TiO₂/HZSM-5(500) 60 wt%.

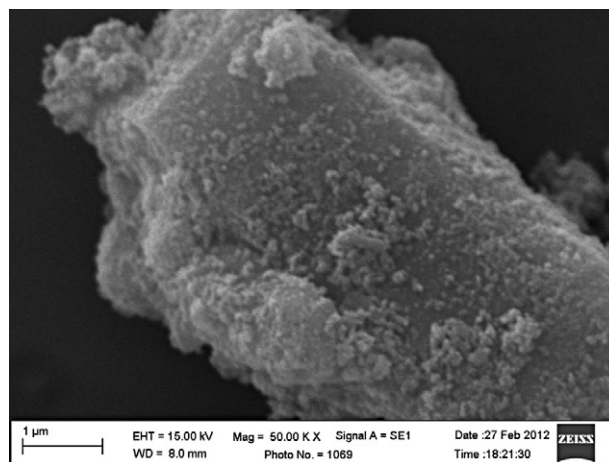


Fig. 4. SEM images of TiO₂ hybridized with HZSM-5 zeolite (TiO₂/HZSM-5(500) 60 wt%).

slightly at around 200–380 nm, indicating that TiO₂ particles are dispersed on the surface of microporous HZSM-5 zeolite powders and the HZSM-5 powders are highly transparent that allow the incident light to penetrate them onto the surface of TiO₂ nano-particles.

The FT-IR spectra of the HZSM-5 with different Si/Al ratios were recorded in the range of 4000–400 cm⁻¹ (Fig. 6). FT-IR spectra showed distinctly sharp absorption bands at 3650, 3420 and 1620 cm⁻¹, which were respectively assigned to “free” –OH stretching vibration [27], hydroxyl stretching vibration of molecularly adsorbed water [20], and HOH deformational vibration of molecular water [27]. The results exhibited that HZSM-5(25) could easily adsorb water molecules and condense them in the zeolite cavities, indicating that the zeolites with lower Si/Al ratios performed higher hydrophilicity. However, highly siliceous HZSM-5(500) zeolite performed a hydrophobicity, which prevented water condensation in the zeolite cavities. The strong absorption band in the region of 1100–1050 cm⁻¹ was assigned to the internal vibration of Si(OH)Al tetrahedral of ZSM-5[28].

3.2. Transient behavior

As shown in Fig. 7, the transient behavior of photocatalytic oxidation of NO_x on TiO₂/HZSM-5(500) 60 wt% was recorded. When the gas concentration in stream was kept at a constant, the

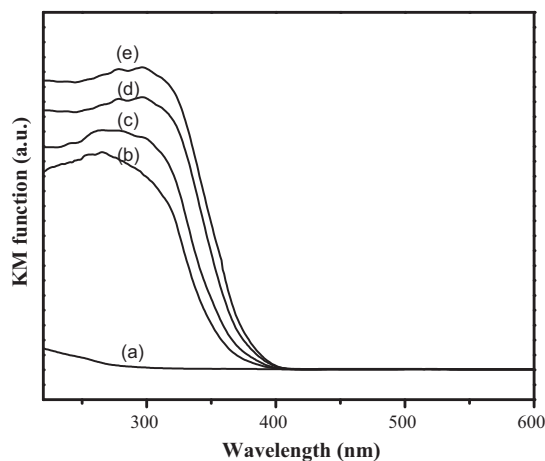


Fig. 5. UV–vis diffuse reflectance spectra of the samples with different zeolite contents. (a) HZSM-5; (b) TiO₂/HZSM-5(500) 80 wt%; (c) TiO₂/HZSM-5(500) 60 wt%; (d) TiO₂/HZSM-5(500) 40 wt%; (e) P25.

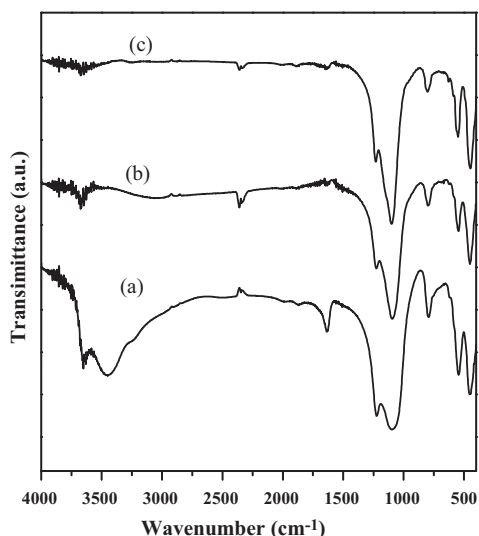


Fig. 6. FT-IR spectra of HZSM-5 zeolites with different Si/Al ratios. (a) 25, (b) 200, and (c) 500.

photocatalytic reaction was initiated. At the beginning, the concentration of NO at the outlet decreased quickly because photo-induced holes were trapped by OH^- or H_2O on the surface of the catalyst, yielding hydroxyl radicals, which were responsible for the chemisorption of NO [6]. The concentration of NO at the outlet increased when the adsorption saturation was achieved and varied little after UV light irradiation for 10 min. The nitrogen equilibrium in the gas phase was reached approximately after 24 h irradiation: $\text{NO}_{\text{out}} (32 \text{ ppm}) + \text{NO}_{2 \text{out}} (6.9 \text{ ppm}) \approx \text{NO}_{\text{in}} (39.6 \text{ ppm})$. Although the nitrogen equilibrium was reached after 24 h, the NO_2 concentration at the outlet began to decrease and the NO concentration increased after 12 h. The decrease of NO_2 yield indicated that the formation of nitrate species occupied the active sites of surface TiO_2 , resulting in the deactivation of the photocatalyst. After washing and calcination treatments, the activity of the $\text{TiO}_2/\text{HZSM-5}$ was recovered and the catalyst could be reused for photocatalytic NO_x oxidation for 5 recycles without deactivation. Compared with the time for pure TiO_2 to reach nitrogen equilibrium in 30 min irradiation, TiO_2 hybridized with HZSM-5 zeolites could largely extend the time to reach nitrogen equilibrium, indicating that the addition of HZSM-5 zeolites resulted in much more production of NO_2^- or NO_3^- ions. This is probably because $\text{TiO}_2/\text{HZSM-5}$ photocatalysts have higher surface areas than pure TiO_2 , preventing the

aggregation of nitrate ions formed at active sites on TiO_2 surface. Accordingly, exposed active sites were responsible for the oxidation of NO_2 to NO_3^- , resulting in that the time to reach nitrogen equilibrium was largely extended. In view of NO reaching steady state in 30 min over TiO_2 , we defined the NO conversion as: $\text{NO conversion (\%)} = (\text{NO}_{\text{in}} - \text{NO}_{\text{out at 30 min}}) / \text{NO}_{\text{in}} \times 100\%$.

3.3. Effect of zeolite content

Fig. 8 shows the effect of different zeolite contents on the photocatalytic activity of the catalysts for NO_x oxidation. The amount of TiO_2 was constant for each experiment, so the content of the zeolite was varied to prepare samples having different zeolite contents. This made us investigate the effect of HZSM-5 addition on the photocatalytic activity. It was found that NO conversion increased with the addition of HZSM-5 and reached the highest when the content of zeolite was 60 wt%. The enhancement of photocatalytic activity may be attributed to the largely increased surface area of the $\text{TiO}_2/\text{HZSM-5}$ photocatalysts compared with that of pure TiO_2 . In many cases, the improvement of surface area is prone to enhance photocatalytic activity of catalysts in gas phase. However, a further increase in the amount of HZSM-5 resulted in the decrease in the NO conversion. This could imply that excess HZSM-5 can decrease the contact efficiency between reactant and active sites on the surface of catalysts. While the yield of NO_2 decreased with the increase in the addition amount of HZSM-5. Katoh et al. reported that NO_2 could interact strongly with the acidic sites of HZSM-5 [29]. Therefore, the adsorption ability of NO_2 on the composite was improved with the increase in the addition of zeolite, resulting in further photooxidation of NO_2 to HNO_3 . This result indicated that the enhancement of adsorption ability is responsible for reduction of NO_2 yield. The results notably exhibited that the combination between TiO_2 and HZSM-5 zeolites could not only elevate NO removal but also inhibit the yield of intermediate (NO_2) formation.

3.4. Effect of adsorption time in dark

As reported in many papers [6,10,30], the oxidation of NO_x on TiO_2 materials easily proceeds in the existence of water vapor, however, the effect of water vapor on the photocatalytic activity of TiO_2 hybridized with zeolites for NO_x oxidation is not understood. As shown in Fig. 9, the effect of pre-adsorption of the inlet gases involving water vapor on the photocatalytic activity of $\text{TiO}_2/\text{HZSM-5}$ for NO_x oxidation was investigated. With the increase in the adsorption time in dark, the NO conversion on TiO_2 hybridized

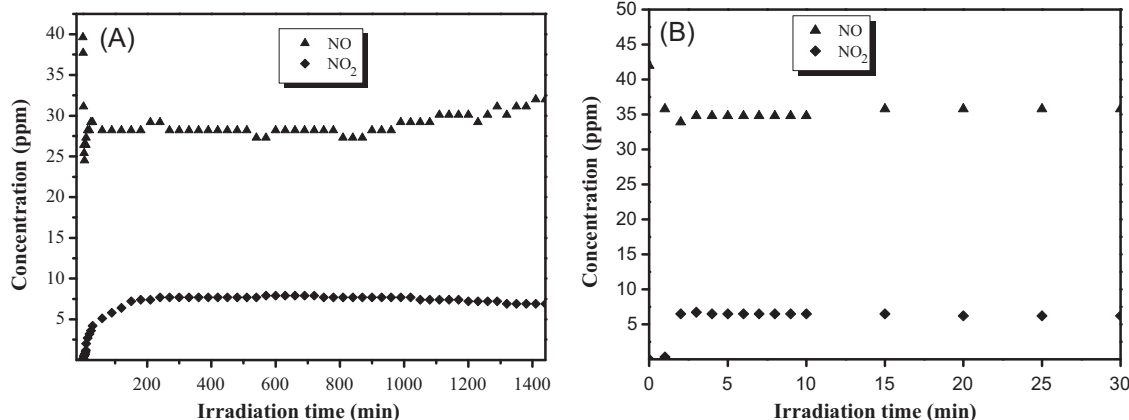


Fig. 7. (A) Transient behavior of $\text{TiO}_2/\text{HZSM-5}(500)$ during 24 h of operation and (B) transient behavior of TiO_2 during of 30 min of operation (relative humidity: 70%; adsorption time in dark: 10 min; zeolite content: 60 wt%).

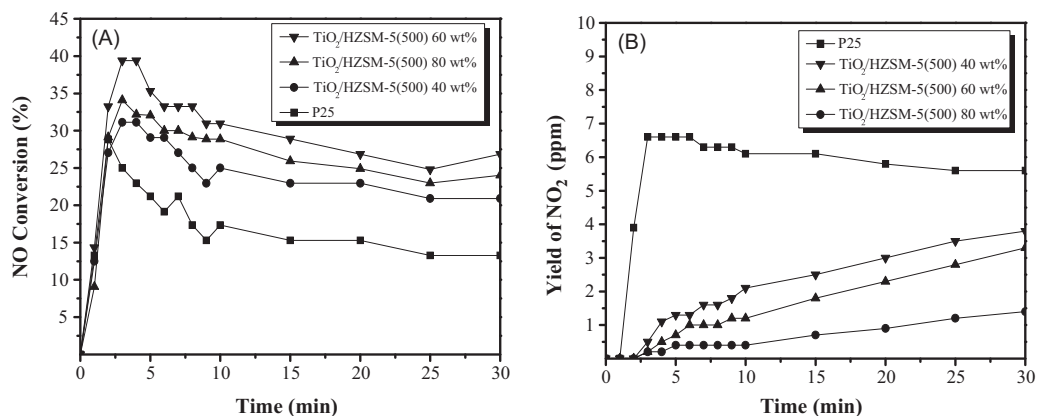


Fig. 8. Photocatalytic reactivity of samples with different zeolite contents: (A) NO conversion and (B) yield of NO₂ (relative humidity: 70%; adsorption time in dark: 10 min).

with hydrophilic HZSM-5 with low Si/Al ratios decreased, while the conversion varied little over TiO₂ hybridized with hydrophobic HZSM-5 with high Si/Al ratio and TiO₂, indicating that the photocatalytic efficiency of NO_x oxidation over TiO₂ hybridized with highly hydrophilic zeolites was largely affected by adsorption time in dark at high levels of humidity. The photocatalytic activity of hydrophobic HZSM-5(500) zeolite hybridized with TiO₂ was better than that of pure TiO₂ even after 30 min adsorption in dark, while hydrophilic HZSM-5(25) combined with TiO₂ showed lower activity than pure TiO₂ after 10 min adsorption in dark. It is presumed that water condenses in zeolite cavities prior to photocatalysis, which leads to the decrease in adsorption sites. As a result, the photocatalytic activity of the hybridized hydrophilic zeolite catalyst for NO_x oxidation decreased.

3.5. Effect of humidity

The effect of relative humidity on photocatalytic activity of TiO₂/HZSM-5 with different Si/Al ratios for NO_x oxidation is shown in Fig. 10. All of the TiO₂/HZSM-5 composite catalysts exhibited much higher NO conversion and lower NO₂ formation than pure TiO₂ in a wide range of relative humidity from 3.5% to 70%. The NO conversion on hydrophobic HZSM-5(500) hybridized with TiO₂ decreased 17% with the relative humidity increased from 3.5% to 70%, while the NO conversion on hydrophilic HZSM-5(25) combined with TiO₂ drastically dropped 40% when the humidity was elevated from 3.5% to 10% and varied unapparently when the relative humidity was higher than 10%. For P25 TiO₂, the NO conversion and the yield of NO₂ increased with the increase in the

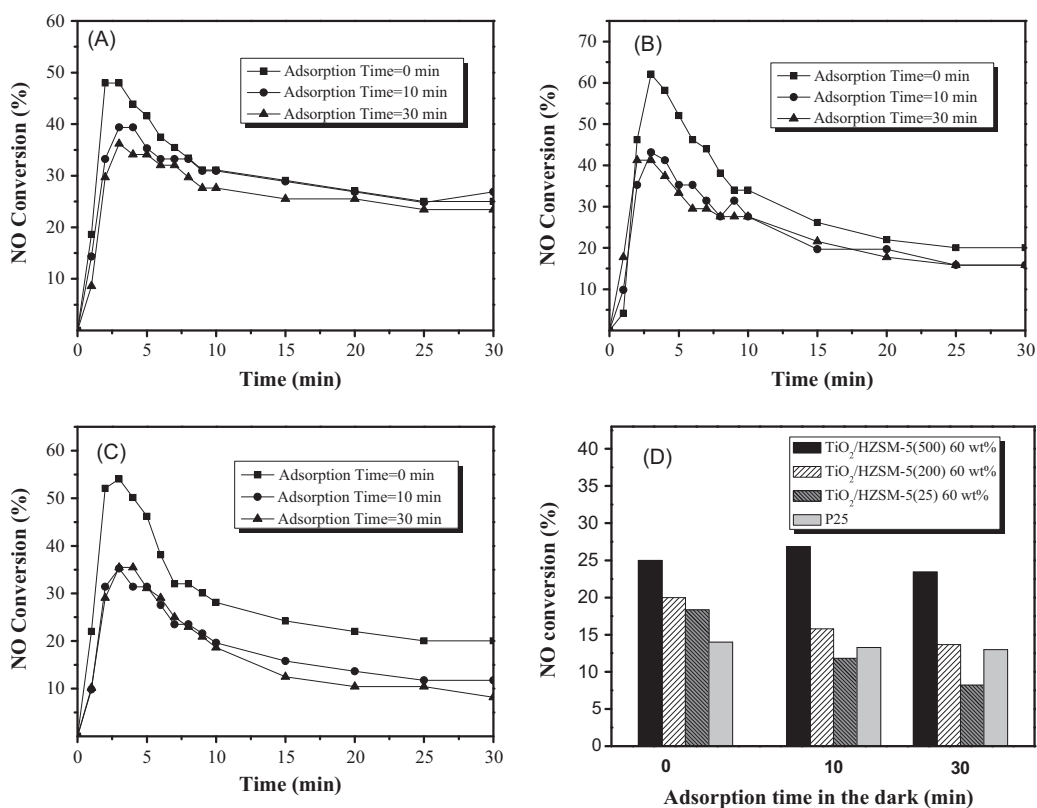


Fig. 9. Effect of adsorption time in dark on photocatalytic activity of TiO₂/HZSM-5: (A) TiO₂/HZSM-5(500); (B) TiO₂/HZSM-5(200); (C) TiO₂/HZSM-5(25); (D) NO conversion vs. adsorption time (relative humidity: 70%; zeolite content: 60 wt%).

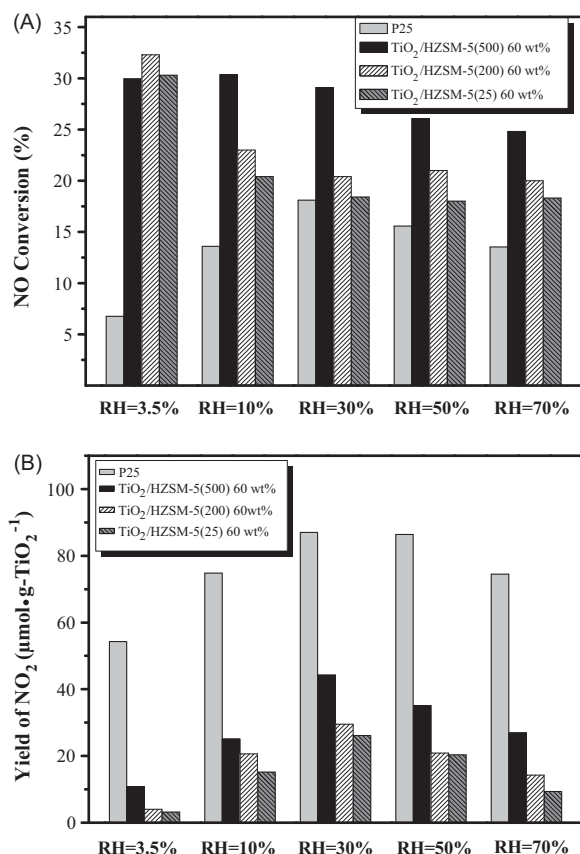


Fig. 10. Effect of relative humidity on photocatalytic reactivity of TiO₂/HZSM-5 with different Si/Al ratios and TiO₂ for NO_x oxidation: (A) NO conversion and (B) yield of NO₂ (adsorption time in dark: 0 min; zeolite content: 60 wt%).

humidity first and then decreased with further increase in humidity from 30%, which may be resulted from the competitive adsorption between water vapor and the reactants (NO and NO₂) [31]. These results indicated that a bit of water vapor gradually condenses in hydrophobic zeolite cavities, but it quickly saturates in hydrophilic zeolite with the increase of water vapor in gas stream, resulting in the decrease in available active sites and adsorption capacity to the gaseous reactants, followed by a decrease in the NO conversion. When water vapor saturated in hydrophilic zeolite cavities, the NO conversion changed unapparently with further increase of water vapor in gas stream. However, the NO₂ production was elevated as the relative humidity increased to 30%, and dropped with further increase in the relative humidity. It may elucidate that the water condensed in zeolite cavities might interact with NO₂, resulting in less yield of NO₂. The result that hydrophilic zeolite hybridized with TiO₂ yielded less NO₂ than hydrophobic zeolite composite also demonstrated that condensed water in zeolite cavities interacted with NO₂.

3.6. Discussion

The reaction mechanism proposed by Devahasdin et al. [6] and Dalton et al. [7] is applied to demonstrate the above results, as depicted in Fig. 11. When the humidity increases from 4% to 30%, the amount of HO• radical increases with water on the surface of pure TiO₂, leading to higher NO conversion and NO₂ yield. However, catalysts of TiO₂ hybridized with zeolite produce more HO• radicals even at low humidity due to adequate adsorption of water vapor, which makes NO conversion keep at high level and NO₂ increase accordingly. When the humidity increases from 30% to 70%, excess

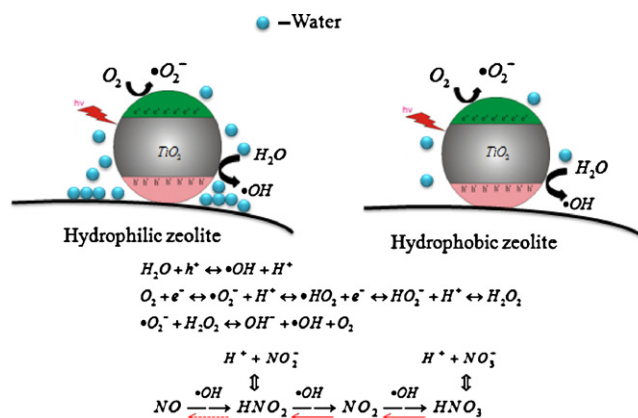


Fig. 11. The graphical illustration of reaction mechanism.

of water may compete with HO• radicals on the surface of pure TiO₂, resulting in lower activity. As for TiO₂ hybridized with hydrophobic zeolite catalyst, the NO conversion varies little because hydrophobicity of zeolite can remarkably inhibit the condensation of water in the cavities, so the effect of water on photocatalytic activity of such catalyst is not obvious. However, as for TiO₂ hybridized with hydrophilic zeolite, water vapor quickly saturates around the active sites with increasing of humidity, leading to notable dropping of NO conversion. Meanwhile, excess water condenses around the surface of TiO₂ hybridized with zeolite sample, resulting in an accelerated disassociation of HNO₂ and HNO₃ which are produced from NO₂ conversion.

4. Conclusions

TiO₂ hybridized with HZSM-5 zeolites photocatalysts were prepared by a simple solid state dispersion method. The TiO₂/HZSM-5 catalysts exhibited higher photocatalytic reactivity for NO_x oxidation compared with the pure TiO₂. The combination between TiO₂ and HZSM-5 zeolites not only improved NO removal efficiency but also inhibited the yield of intermediate (NO₂) formation. The highest NO conversion was found on the composite catalyst with zeolite content of 60 wt%, while the yield of NO₂ decreased with the addition of HZSM-5, which might be attributed to the largely increased surface area of the composite catalysts and the optimal contact efficiency between reactant and active sites as well as the strong adsorption ability of NO₂ on HZSM-5. TiO₂ hybridized with hydrophobic HZSM-5 zeolite retained high photocatalytic reactivity in a wide range of relative humidity and water pre-adsorption time. However, the pre-adsorption with water vapor and the high humidity during the photoreaction were harmful to the reactivity of TiO₂ hybridized with hydrophilic zeolite. The results suggested an important role of the hydrophobicity of zeolite on the photocatalytic reactivity of TiO₂/HZSM-5 catalysts for NO_x oxidation.

Acknowledgments

This work was supported by National Natural Science Foundation of China (Nos. 20807015, 21037001), Ph.D. The Science and Technology Project of Guangzhou City (No. 12C62081602), Programs Foundation of Ministry of Education of China (No. 200805611055), and the Fundamental Research Funds for the Central Universities, SCUT (No. 2012ZZ0049).

References

- [1] T. Ibusuki, K. Takeuchi, Removal of low concentration nitrogen oxides through photoassisted heterogeneous catalysis, *J. Mol. Catal.* 88 (1994) 93–102.
- [2] A. Fujishima, X. Zhang, D. Tryk, TiO₂ photocatalysis and related surface phenomena, *Surf. Sci. Rep.* 63 (2008) 515–582.

- [3] Z.B. Wu, Z.Y. Sheng, Y. Liu, H.Q. Wang, N. Tang, J. Wang, Characterization and activity of Pd-modified TiO₂ catalysts for photocatalytic oxidation of NO in gas phase, *J. Hazard. Mater.* 164 (2009) 542–548.
- [4] H. Ichiura, T. Kitaoka, H. Tanaka, Removal of indoor pollutants under UV irradiation by a composite TiO₂-zeolite sheet prepared using a papermaking technique, *Chemosphere* 50 (2003) 79–83.
- [5] S. Rehman, R. Ullah, A. Butt, N. Gohar, Strategies of making TiO₂ and ZnO visible light active, *J. Hazard. Mater.* 170 (2009) 560–569.
- [6] S. Devahasdin, C. Fan, K.Y. Li, D.H. Chen, TiO₂ photocatalytic oxidation of nitric oxide: transient behavior and reaction kinetics, *J. Photochem. Photobiol. A* 156 (2003) 161–170.
- [7] J. Dalton, P. Janes, N. Jones, J. Nicholson, K. Hallam, G. Allen, Photocatalytic oxidation of NO_x gases using TiO₂: a surface spectroscopic approach, *Environ. Pollut.* 120 (2002) 415–422.
- [8] C.H. Ao, S.C. Lee, Enhancement effect of TiO₂ immobilized on activated carbon filter for the photodegradation of pollutants at typical indoor air level, *Appl. Catal. B: Environ.* 44 (2003) 191–205.
- [9] M. Litter, Heterogeneous photocatalysis: transition metal ions in photocatalytic systems, *Appl. Catal. B: Environ.* 23 (1999) 89–114.
- [10] M. Takeuchi, T. Kimura, M. Hidaka, D. Rakhmawaty, M. Anpo, Photocatalytic oxidation of acetaldehyde with oxygen on TiO₂/ZSM-5 photocatalysts: effect of hydrophobicity of zeolites, *J. Catal.* 246 (2007) 235–240.
- [11] M. Signoretto, E. Ghedini, V. Trevisan, C. Bianchi, M. Ongaro, G. Cruciani, TiO₂-MCM-41 for the photocatalytic abatement of NO_x in gas phase, *Appl. Catal. B: Environ.* 95 (2009) 130–136.
- [12] X. Huang, J. Yuan, J. Shi, W. Shangguan, Ozone-assisted photocatalytic oxidation of gaseous acetaldehyde on TiO₂/H-ZSM-5 catalysts, *J. Hazard. Mater.* 171 (2009) 827–832.
- [13] M. Phanikrishna Sharma, V. Durga Kumari, M. Subrahmanyam, TiO₂ supported over porous silica photocatalysts for pesticide degradation using solar light. Part 2. Silica prepared using acrylic acid emulsion, *J. Hazard. Mater.* 175 (2010) 1101–1105.
- [14] C.H. Ao, S.C. Lee, Combination effect of activated carbon with TiO₂ for the photodegradation of binary pollutants at typical indoor air level, *J. Photochem. Photobiol. A* 161 (2004) 131–140.
- [15] S. Yuan, Q.R. Sheng, J.L. Zhang, H. Yamashita, D.N. He, Synthesis of thermally stable mesoporous TiO₂ and investigation of its photocatalytic activity, *Micropor. Mesopor. Mater.* 110 (2008) 501–507.
- [16] A.C. Lee, R.H. Lin, C.Y. Yang, M.H. Lin, W.Y. Wang, Preparations and characterization of novel photocatalysts with mesoporous titanium dioxide (TiO₂) via a sol-gel method, *Mater. Chem. Phys.* 109 (2008) 275–280.
- [17] N. Chen, Hydrophobic properties of zeolites, *J. Phys. Chem.* 80 (1976) 60–64.
- [18] L. Liao, W. Wu, C. Chen, J. Lin, Photooxidation of formic acid vs formate and ethanol vs ethoxy on TiO₂ and effect of adsorbed water on the rates of formate and formic acid photooxidation, *J. Phys. Chem. B* 105 (2001) 7678–7685.
- [19] K. Miller, C. Lee, J. Falconer, J. Medlin, Effect of water on formic acid photocatalytic decomposition on TiO₂ and Pt/TiO₂, *J. Catal.* (2010).
- [20] L. Cao, A. Huang, F. Spiess, S. Suib, Gas-phase oxidation of 1-butene using nanoscale TiO₂ photocatalysts, *J. Catal.* 188 (1999) 48–57.
- [21] T. Obee, R. Brown, TiO₂ photocatalysis for indoor air applications: effects of humidity and trace contaminant levels on the oxidation rates of formaldehyde, toluene, and 1,3-butadiene, *Environ. Sci. Technol.* 29 (1995) 1223–1231.
- [22] T. Liu, F. Li, X. Li, TiO₂ hydrosols with high activity for photocatalytic degradation of formaldehyde in a gaseous phase, *J. Hazard. Mater.* 152 (2008) 347–355.
- [23] K. Hashimoto, K. Wasada, M. Osaki, E. Shono, K. Adachi, N. Toukai, H. Kominami, Y. Kera, Photocatalytic oxidation of nitrogen oxide over titania-zeolite composite catalyst to remove nitrogen oxides in the atmosphere, *Appl. Catal. B: Environ.* 30 (2001) 429–436.
- [24] V. Durgakumari, M. Subrahmanyam, K. Subba Rao, A. Ratnamala, M. Noorjahan, K. Tanaka, An easy and efficient use of TiO₂ supported HZSM-5 and TiO₂ + HZSM-5 zeolite combine in the photodegradation of aqueous phenol and p-chlorophenol, *Appl. Catal. A: Gen.* 234 (2002) 155–165.
- [25] A. Neren Ökte, Özge Yilmaz, Photodecolorization of methyl orange by yttrium incorporated TiO₂ supported ZSM-5, *Appl. Catal. B: Environ.* 85 (2008) 92–102.
- [26] M. Ali, B. Brisdon, W. Thomas, Synthesis, characterization and catalytic activity of ZSM-5 zeolites having variable silicon-to-aluminum ratios, *Appl. Catal. A: Gen.* 252 (2003) 149–162.
- [27] M. Nagao, Y. Suda, Adsorption of benzene, toluene, and chlorobenzene on titanium dioxide, *Langmuir* 5 (1989) 42–47.
- [28] H.G. Karge, J. Weitkamp, *Molecular Sieves: Science and Technology*, vol. 4, 2004, p. 99.
- [29] M. Katoh, T. Yamazaki, H. Kamijo, S. Ozawa, Infrared studies on nitrogen oxides adsorbed on alkali metal ion-exchanged ZSM-5 zeolites, *Zeolites* 15 (1995) 591–596.
- [30] H.Q. Wang, Z.B. Wu, W.R. Zhao, B.H. Guan, Photocatalytic oxidation of nitrogen oxides using TiO₂ loading on woven glass fabric, *Chemosphere* 66 (2007) 185–190.
- [31] H. Tawara, Development of evaluation method of air-purifying paving blocks for NO_x removal capacity, in: *Proceedings of the Fourth International Conference on TiO₂ Photocatalytic Purification and Treatment of Water and Air*, Albuquerque, 1999, pp. 24–28.